Polish Journal of Chemical Technology, 18, 1, 93—98, 10.1515/pjct-2016-0014

Kinetic study of CO_2 reaction with CaO by a modified random pore model

S.M.M. Nouri[1*], H. Ale Ebrahim[2]

[1]*Hakim Sabzevari University, Chemical Engineering Department, Sabzevar, 9617976487, Iran*
[2]*Amirkabir University of Technology, Chemical Engineering Department, Petrochemical Centre of Excellency, Tehran, 15875-4413, Iran*
[*]*Corresponding author: e-mail: m.nouri@hsu.ac.ir*

In this work, a modified random pore model was developed to study the kinetics of the carbonation reaction of CaO. Pore size distributions of the CaO pellets were measured by nitrogen adsorption and mercury porosimetry methods. The experiments were carried out in a thermogravimeter at different isothermal temperatures and CO_2 partial pressures. A fractional concentration dependency function showed the best accuracy for predicting the intrinsic rate of reaction. The activation energy was determined as 11 kcal/mole between 550–700°C. The effect of product layer formation was also taken into account by using the variable product layer diffusivity. Also, the model was successfully predicted the natural lime carbonation reaction data extracted from the literature.

Keywords: carbonation reaction, calcium oxide, mathematical modeling, random pore model, pore size distribution.

INTRODUCTION

Carbon dioxide emission continued an upward trend in the 21st century. Fossil fuels are responsible for more than 75% of anthropogenic CO_2 emission[1]. Carbon dioxide capture using calcium oxide in a carbonation/calcination cycle is one of the promising methods to remove CO_2 from flue gas of stationary sources[2]. This process has attracted so much attention due to its advantages with respect to other well-known processes such as amine-based absorption. The cheap sorbents and high temperature nature of carbonation and calcination reactions reduce the efficiency penalty which it imposes upon a power station to about 6–8% including CO_2 compression[3]. Also, circulating fluidized bed reactors are suitable for large scale capture process[4, 5, 6].

Bhatia and Perlmutter[7] studied the carbonation reaction and proposed a random pore model which exploits a relationship between the actual volume of the porous matrix and ideal volume in the absence of pore intersections. Their model also considers diffusion and transport effects, including the buildup of product layer. Khoshandam et al developed a grain model to predict the carbonation reaction behavior[8]. Sun et al used grain model to obtain kinetic constants for calcined limestone and dolomite[9]. Their results showed that intrinsic rate have a variable order as a function of CO_2 partial pressure. The same group developed a new gas-solid model based on discrete pore size distribution measurement which successfully predicted their experimental data in a wide range of temperatures and CO_2 partial pressure[10].

Different reaction orders and activation energies were reported by different authors for reaction of CO_2 with calcium oxide. Zero activation energy for surface reaction was obtained by Nitsch and further supported by Bhatia and Perlmutter and Dennis and Hayhurst[7, 11, 12]. The uncertainty of intrinsic reaction order is another issue with respect to carbonation reaction. Sun et al found that reaction rate has a variable order as a function of CO_2 partial pressure[9]. For CO_2 partial pressures of less than 10 kPa, the reaction rate was first order. For higher partial pressures, however, it was found to be zero order. On the other hand, Grasa et al obtained first order reaction for CO_2 partial pressures up to 1 atm by using conventional random pore model[13].

In this work, the kinetics of carbonation reaction was investigated using three different limes including initial CaO, a calcium oxide from $CaCO_3$ calcination and natural lime[13]. The experiments were carried out in a thermogravimeter analyzer (TGA) between 550–700°C and 7–50% CO_2/N_2. The conventional random pore model with accounting a pore size distribution for solid reactant, diffusion in the pores and through product layer and diminishing porosity during the reaction was selected as the basic mathematical model. The last item is due to high molar volume ratio of solid product ($CaCO_3$) with respect to solid reactant (CaO) in this reaction. The random pore model was modified for consideration of the bulk flow effect, and a general concentration dependency. Moreover, the dense $CaCO_3$ product layer formation caused a sudden shift in the reaction rate slopes, and thus the variable product layer diffusivity was used in the random pore model. Consequently, the inherent kinetic constants for the $CaO+CO_2$ reaction can be evaluated accurately.

EXPERIMENTAL PROCEDURE

Two types of starting materials were used: a) calcium oxide (Merck Art. No.102109) and b) calcium carbonate (Merck Art. No.102059). Since calcium oxide was in the small lumps form, it was crushed, powdered and sieved to the mesh size of 200. The slab pellets were made by pressing CaO and $CaCO_3$ powder at 5 MPa in a cylindrical die with 10 mm diameter and 1 mm thickness.

The system used for the experiments consists of a TGA from Rheometric Scientific (model STA-1500). High purity CO_2 and nitrogen were used for the experiments. The pellet is put on a platinum basket cell in the TGA. The system is heated under an inert gas stream (gas 1) with the rate of 20°C/min, up to the desired isothermal operating temperature. After five minutes, the system is switched to a reacting gas mixture (a predefined CO_2/N_2 mixture) as gas 2 and reaction begins at the desired temperature. At this condition, the weight changes are obtained versus time by TGA at a constant temperature.

The total gas flow rate was increased until no change in the conversion-time data was observed. Therefore,

the gas phase mass transfer resistance was eliminated in the overall controlling mechanisms of the reaction.

The nitrogen adsorption and mercury porosimetry were used to evaluate the pore size distributions of the samples (pellets after calcinations and decomposition). Nitrogen adsorption (by Autosorb-1MP from Quantachrome) determines the porous structure in the range of micro and meso pores by a 55 point test. However, larger macro pores that are out of the detection range of nitrogen adsorption can be determined by mercury porosimetry. By using both of above methods and combining their results, the whole pore size distributions in the range of 0.3–10 000 nm can be evaluated. However, the preliminary nitrogen adsorption tests on the initial and partially reacted CaO pellets showed a negligible contribution of micro pores (from HK model) in the reaction with CO_2. Therefore, the volume pore size distribution was determined according to the BJH model (for meso pores) by nitrogen adsorption, and Washburn equation (for macro pores) by mercury porosimetry. Then the random pore model parameters were determined from the above mentioned whole pore size distribution of the solid reactant pellet.

MODEL DEVELOPMENT

The random pore model presented here is a modified version of the model developed by Bhatia and Perlmutter[13] with the following assumptions.

Consider the reaction:

$$A(g)+\vartheta_B B(s)\rightarrow \vartheta_C C(g)+\vartheta_D D(s) \tag{1}$$

1 – The system is isothermal.

2 – The pseudo steady state approximation is valid for gas diffusion in the solid.

3 – The slab pellet thickness is constant.

4 – The bulk gas concentration is constant in the TGA.

5 – Bulk flow effect through the pellet is also considered.

6 – A general concentration dependency is accounted.

7 – Variable product layer diffusivity is considered.

For a pellet with slab geometry, the mass balance for gaseous reactant A is:

$$\frac{d}{dz}(N_A)=R_A \tag{2}$$

Where R_A is the local rate of consumption of the fluid reactant A per unit volume. The molar flux N_A is given by:

$$N_A=(N_A+N_C)x_A-D_E C_T\nabla x_A \tag{3}$$

And from the stoichiometry:

$$N_A=-\upsilon_C N_C \tag{4}$$

Substituting equation (4) in equation (3) and rearranging, we get:

$$N_A=\frac{-D_E C_T\, dx_A/dz}{1-(1-\upsilon_C)x_A} \tag{5}$$

Combining equation (2) and (5), we obtain:

$$\frac{d}{dz}\left[D_e C_T\frac{dx/dz}{1-(1-\upsilon_C)x_A}\right]-R_A=0 \tag{6}$$

So, the modified random pore model dimensionless equations are expressed as follows[14]:

$$\frac{\partial}{\partial y}\left(\frac{\delta}{1+\theta a}\frac{\partial a}{\partial y}\right)=\frac{\phi^2 f(a) b\sqrt{1-\psi\ln b}}{1+\frac{\beta Z}{\psi}\left(\sqrt{1-\psi\ln b}-1\right)} \tag{7}$$

$$\frac{\partial b}{\partial \tau}=-\frac{f(a) b\sqrt{1-\psi\ln b}}{1+\frac{\beta Z}{\psi}\left(\sqrt{1-\psi\ln b}-1\right)} \tag{8}$$

Which the initial and boundary conditions are:

$$\begin{aligned}&\tau=0\rightarrow\ b=1\\ &y=0\rightarrow\ \frac{\partial a}{\partial y}=0\\ &y=1\rightarrow\ a=1\end{aligned} \tag{9}$$

In these equations, ψ is the random pore model parameter which is a function of initial pore size distribution of the pellet, â is the modified Biot modulus presenting the product layer diffusion resistance, f(a) is the concentration dependency function, and Z is the molar volume ratio of the solid product to the solid reactant as follows:

$$Z=\frac{\vartheta_D \rho_B M_D}{\vartheta_B \rho_D M_B} \tag{10}$$

The molar volume ratio of calcium carbonate to calcium oxide for carbonation reaction is 2.17. The structural parameters of the model can be calculated from the pore volume distribution functions as follows[7]:

$$\varepsilon_0=\frac{V_p}{V_p+1/\rho_B} \tag{11}$$

$$S_0=2(1-\varepsilon_0)\int_0^\infty\frac{dv_0}{r(1-v_0)} \tag{12}$$

$$L_0=\frac{1-\varepsilon_0}{\pi}\int_0^\infty\frac{dv_0}{r^2(1-v_0)} \tag{13}$$

$$\psi=\frac{4\pi L_0(1-\varepsilon_0)}{S^2} \tag{14}$$

The equation suggested by Wakao and Smith is used to obtain the pore diffusion as a function of pellet porosity[15]:

$$\delta=\frac{D_e}{D_{e0}}=\left(\frac{\varepsilon}{\varepsilon_0}\right)^2=\left[1-\frac{(Z-1)(1-\varepsilon_0)(1-b)}{\varepsilon_0}\right]^2 \tag{15}$$

The effective initial diffusivity of the reactant gas through the lime pores can be obtained as follows:

$$\frac{1}{D_{e0}}=\frac{1}{\varepsilon_0^2}\left(\frac{1}{D_{AM}}+\frac{1}{D_{AK}}\right) \tag{16}$$

Where D_{AM} is the molecular diffusivity and is estimated from Slattery and Bird[16] equation. D_{AK} is the Knudsen diffusivity and can be calculated as[17]:

$$D_{AK}=9700\times\frac{2\varepsilon_0}{S_0}\left(\frac{T}{M_w}\right)^{0.5} \tag{17}$$

RESULTS

The pore size distributions of both sorbents are shown in Figure 1. As can be seen in this figure, calcined calcium carbonate shows bigger pore sizes than calcium oxide pellet especially at macro-pore region. It seems that during the calcination process, the porosity of calcium carbonate pellet increases respectively due to losing the CO_2 molecules. The structural parameters of

the sorbents are shown in Table 1 for the two calcium oxide pellets used in this work and calcined limestone from the experiments of Grasa[13].

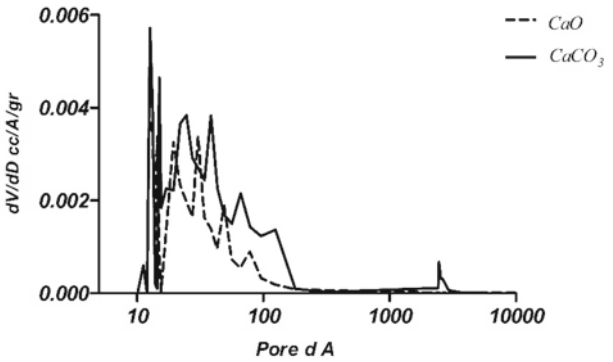

Figure 1. Pore size distributions for the two different reactant samples (CaO and calcined $CaCO_3$) measured by nitrogen adsorption and mercury porosimetry

The effect of bulk flow on the reaction conversion is shown in Figure 2. Because there is no product gas for carbonation reaction of carbon dioxide with calcium oxide ($\theta<0$), the inward bulk flow speeds up the diffusion, thus increasing the overall rate of reaction. Therefore, neglecting the bulk flow effect in kinetic study of non-equimolar counter-diffusion reactions poses some error in rate constants.

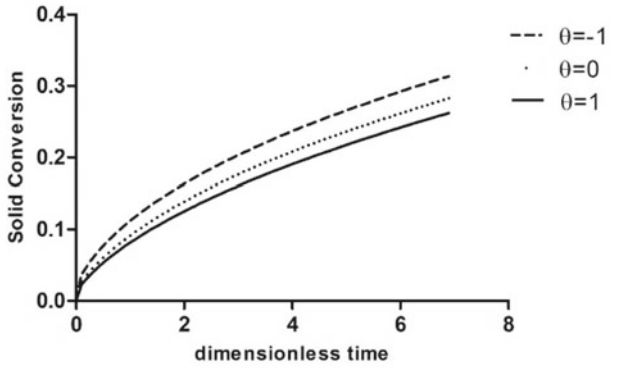

Figure 2. Effect of bulk flow on the conversion-time profiles. Sh = 1, Φ = 4, ψ = 1.1, ε_0 = 0.35, β = 2 ($\theta > 0$ product gas, $\theta = 0$ equimolar counter flow, $\theta < 0$ reactant gas)

Figures 3 shows some conversion-time data at various temperatures and CO_2 concentrations obtained from TGA for calcined $CaCO_3$ and initial CaO pellets respectively. As seen in Figure 3 for calcined $CaCO_3$ pellet, after an initial rapid growth, there is a sudden transition to a much slower reaction rate regime. But for initial CaO pellet, there is a short kinetic control regime for reaction and after that, diffusion controls the overall reaction and the rate decreases sequentially. Moreover, the final conversion of the calcined $CaCO_3$ pellet for

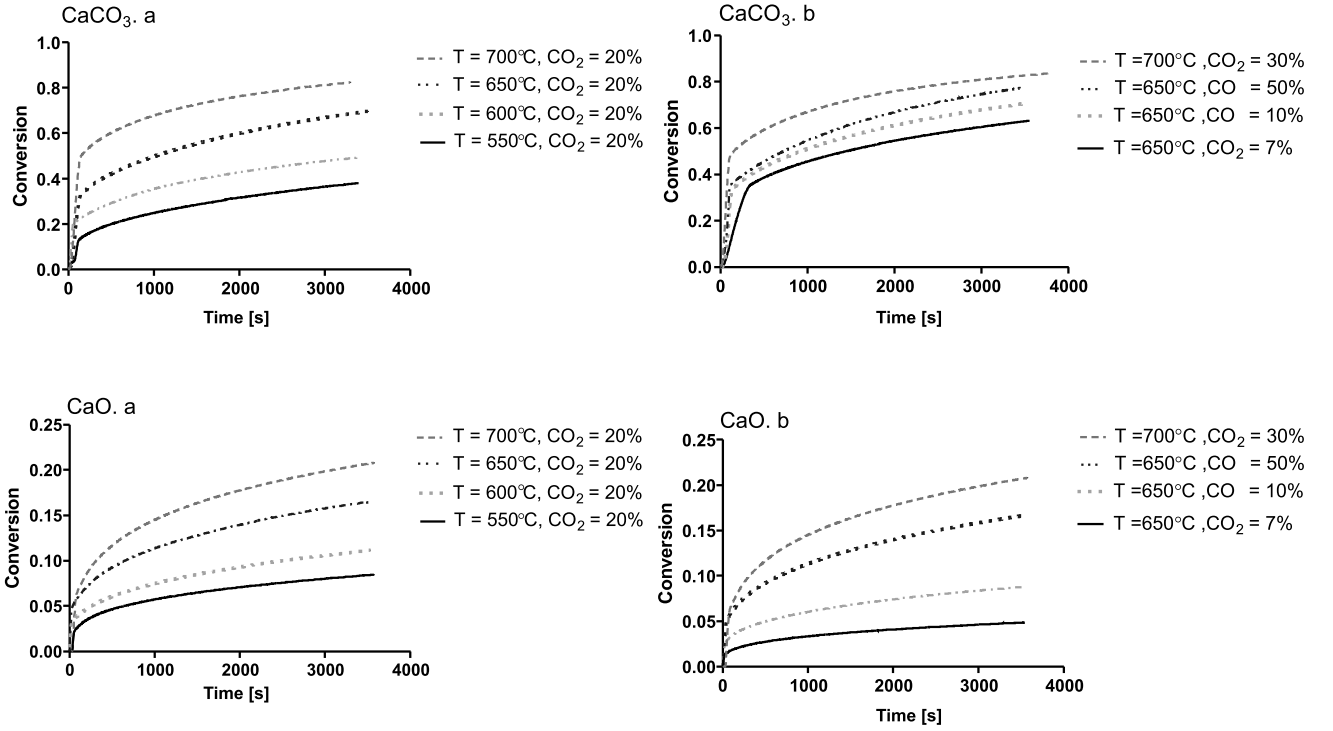

Figure 3. Experimental conversion-time profiles at different temperatures and CO_2 concentrations for CaO from calcined $CaCO_3$ and original CaO

Table 1. Structural parameters of solid reactants for the random pore model

Pellet	$S_0\,(cm^2/cm^3)$	$L_0\,(cm/cm^3)$	Ψ	ε_0
Calcined $CaCO_3$	1.83×10^6	2.05×10^{12}	2.43	0.685
Initial CaO	3.39×10^6	4.61×10^{12}	2.67	0.47
Calcined limestone[13]	4.2×10^5	4.16×10^{10}	1.52	0.47

a similar operating condition is about four times higher than initial CaO pellet sample.

DISCUSSION

It is assumed that for carbonation reaction at initial stage, the diffusion through $CaCO_3$ product layer can be neglected. Thus the intrinsic reaction kinetics and pore diffusion should be considered as controlling mechanisms. At this condition, equations (6) and (7) may be rearranged as:

$$\frac{\partial}{\partial y}\left(\frac{\delta}{1+\theta a}\frac{\partial a}{\partial y}\right)=-\frac{\phi^2\partial b}{\partial \tau} \tag{18}$$

$$\frac{\partial b}{\partial \tau}=-f(a)b\sqrt{1-\psi \ln b} \tag{19}$$

The solid conversion can be computed as:

$$X(\tau)=1-\int_0^1 b(y,\tau)dy \tag{20}$$

The dimensionless solid concentration can be estimated by:

$$b=1-\int_0^1 f(a)d\tau \tag{21}$$

Differentiation of equation (20) yields:

$$\frac{dX}{d\tau}=\int_0^1 f(a)dy \tag{22}$$

The above equation can be rearranged as:

$$\frac{(1-\varepsilon_0)}{S_0\int_0^1 f(a)dy}\left[\frac{dX}{dt}\right]_{t\to 0}=k_s\left(C_A-C_{Aeq}\right)^n \tag{23}$$

The kinetic constants can be calculated by plotting the left hand side of equation (23) from the initial experimental conversion-time slopes, versus C_A^n. Equilibrium concentration of CO_2 was obtained from Barker's work[18]. The above mentioned procedure is repeated for each concentration dependency and the deviation of points from linearity shows the accuracy of the reaction function f(a) for predicting the experimental data. Also the activation energy was evaluated as 11 kcal/mol by fitting kinetic constants to the Arrhenius equation. The results of these computations are shown in Table 2.

It is clear that fractional concentration dependency shows the best accuracy with experimental data. This type of equation presents a near first order reaction at low CO_2 concentrations, and the reaction rate dependency approaches zero order with increase in concentration. Thus, the intrinsic reaction rate concentration dependency is presented as follows:

$$r_A=\frac{k_s a}{1+k_{ad}C_{Ab}a} \tag{24}$$

The obtained fractional reaction rate function is in agreement with some other studies for the kinetics of $CaO+CO_2$ reaction. Bhatia and Perlmutter obtained a first order reaction for CO_2 concentration lower than 10%[7], whereas Kyaw et al claimed a zero order for higher CO_2 partial pressures[19]. Also, Sun et al studied the kinetics of $CaO+CO_2$ reaction using the grain model[9]. They found that the intrinsic rate has a variable order with respect to CO_2 partial pressure, changing from first order to zero order for CO_2 partial pressures greater than 10 kPa.

The low obtained activation energy in this work (11 kcal/mol) is also consistent with the literature results. Sun et al[9] reported an activation energy of 29±4 kJ/mol for calcined limestone, but Kyaw et al[19] obtained 18.6 kcal/mol for activation energy of carbonation reaction. Bhatia and Perlmutter[7] observed no significant trend of rate constants with changes in temperatures.

Bhatia and Perlmutter used an approximate solution to solve the problem of rapid change in experimental conversion-time slopes for the $CaO+CO_2$ reaction[7]. They assumed that for the second stage, the CO_2 concentration is linear across the product layer and then established an approximate equation for this stage. The derived equation predicts the behavior of reaction up to about 50–60% conversion. However, in the present work the product layer diffusivity was assumed as an exponential function of solid conversion as follows:

$$D_p=D_{P0}\exp(-aX^b) \qquad a=4 \qquad b=1.5 \tag{25}$$

$$D_P \quad at \quad X_f=4.1\times 10^{-8}\exp\left(-\frac{32.9\frac{kcal}{mol}}{RT}\right) \tag{26}$$

$R^2 = 0.962$

The values of parameters a and b were obtained using a trial and error method at different temperatures. The above equations are in agreement with findings of Mess et al. They reported that effective product layer diffusivity decreases with time and approaches a constant value for times greater than about 600 min[20]. Also Stendardo et al used the same function for product layer diffusion variation with conversion in the grain model prediction of $CaO+CO_2$ reaction[21].

Figure 4 shows a comparison between the model predictions and experimental data. It can be seen that the modified random pore model predicts the conversion-time data for calcined $CaCO_3$ very well. The initial calcium

Table 2. Deviation of different kinetic functions from equation (18) at different temperatures, and kinetic constants from a fractional concentration dependency function

Degree of reaction	Average R^2	Kinetic constants
N = 1	0.905	
N = 0.5	0.764	
Fractional dependency	0.986	$k_s = 63.43\exp\left(\frac{-11.094\ \text{kcal}/mol}{RT}\right)\ \text{cm}^4/\text{mol}\cdot\text{s}$ $k_{ad} = 10^6\ \text{cm}^3/\text{mol}$

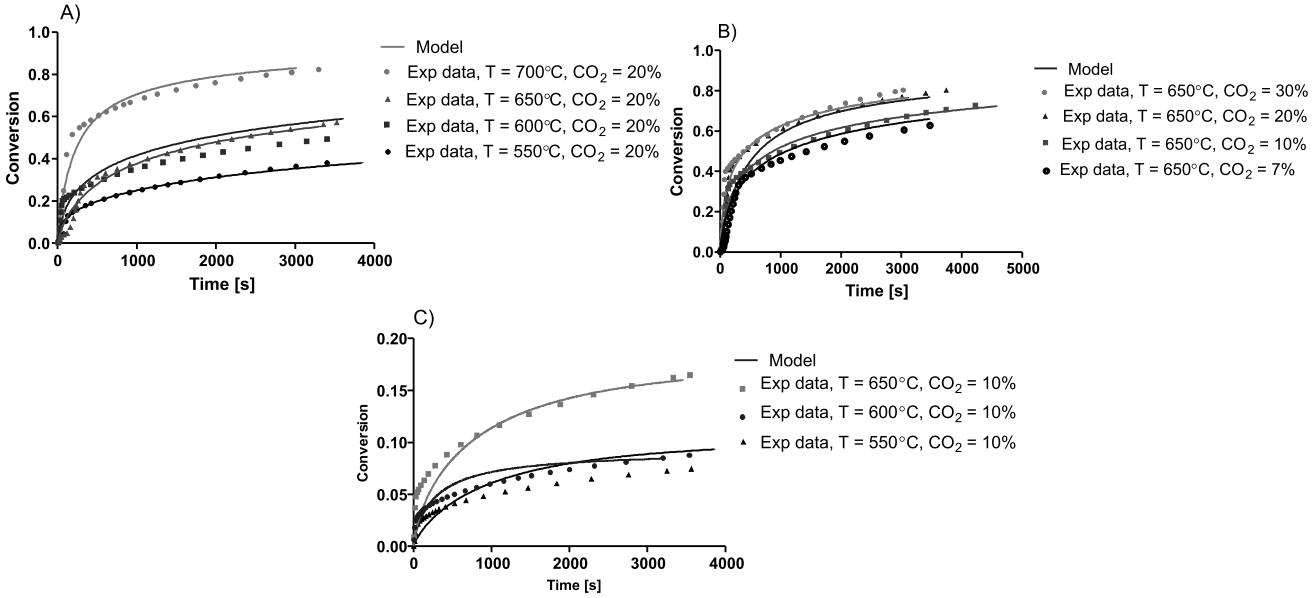

Figure 4. Comparison between experimental data and model predictions at different temperatures and CO_2 concentrations for CaO from CaO (A) and $CaCO_3$ calcination (sample B and C)

oxide pellets, which are less porous than calcined $CaCO_3$, were used to validate the model. As can be seen in Figure 6, the model results are still in agreement with the experimental data for the initial CaO reaction with CO_2.

The carbonation experiments carried out by Grasa[13] were used to validate the model in a practical situation. Figure 5 shows a comparison between the experimental data and the model results for two different temperatures. The model successfully predicts the carbonation reaction behavior for a natural sorbent.

The low value of the effective product layer diffusivity in the range of 10^{-16} cm^2/s, and the high value of its activation energy (33 kcal/mol) of are both consistent with a solid state diffusion hypothesis. But it is still lower than 88 kcal/mol, measured for lattice diffusivities in single crystals of calcite[22]. However, different impurity contents cause different defect structures between product layer calcite and a single crystal.

CONCLUSION

A model for $CaO+CO_2$ reaction was formulated based on the pore size distributions of solid reactant. This reaction is highly sensitive to the porous solid structure. Thus, the pore size distributions are measured by two methods for different pore sizes. It is clear that the random pore model is more accurate than earlier works based on the grain model with a simplification assumption of equal grain sizes. On the other hand, the random pore model was modified for the effects of bulk flow and a general concentration dependency.

The inherent rate constants were calculated by the above mentioned modified random pore model and experimental TGA data at different temperatures. The fractional concentration dependency showed better accuracy than power-law functions with experimental data. This effect can be quite large, increasing with the importance of the product layer diffusion. The diffusion coefficient of CO_2 in product layer was determined as an exponential function of conversion, with an increasing trend while the reaction proceeds. The low value of product layer diffusivity with the high relative activation energy was quite a typical value associated with the solid state diffusion.

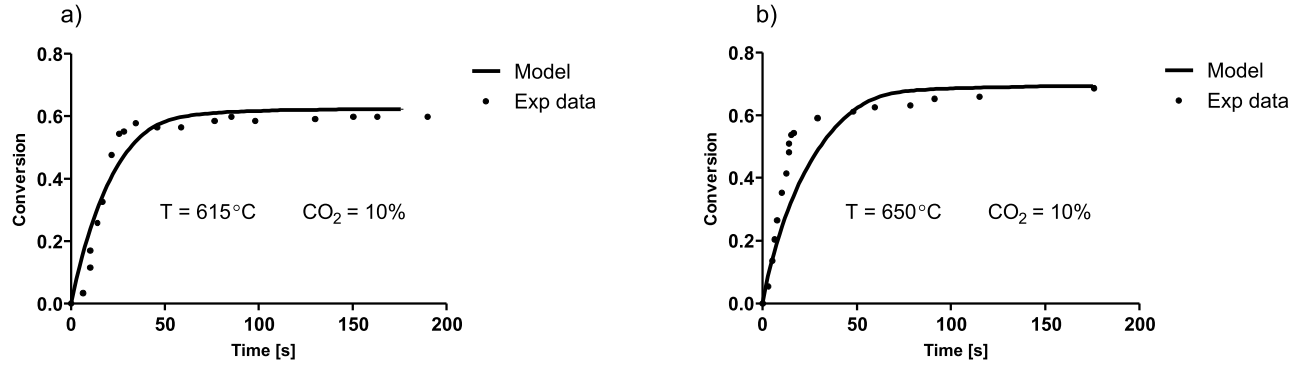

Figure 5. Comparison between experimental data of Grasa [10] and model predictions at different temperatures

NOMENCLATURE

a	C_A/C_{A0}, dimensionless gas concentration
b	C_B/C_{B0}, dimensionless solid concentration
C_A	Gas concentration in the pellet (kmol/m^3)
C_{Ab}	Bulk gas concentration (kmol/m^3)
C_B	solid reactant concentration (kmol/m^3)
C_{B0}	Solid reactant concentration (kmol/m^3)
C_T	Total gas concentration (kmol/m^3)
D_e	Effective diffusivity of gas A in the pellet (m^2/s)
D_{e0}	Initial effective diffusivity of gas A in the pellet (m^2/s)
D_P	Effective diffusivity of gas A in the product layer (m^2/s)
D_{P0}	Initial effective diffusivity of gas A in the product layer (m^2/s)
k_m	External mass-transfer coefficient (m/s)
k_s	Surface rate constant (m^4/kmol · s)
k_{ad}	Adsorption coefficient (m^3/kmol)
M_B	Molecular weight of solid reactant (kg/kmol)
M_D	Molecular weight of solid product (kg/kmol)
r	Distance from the center of the pellet (m)
L_0	Thickness of pellet (m)
S_0	Reaction surface area per unit volume (m^2/m^3)
Sh	Sherwood number for external mass transfer (k_mR_0/D_{e0})
T	Temperature (k)
t	Time (s)
$v_0(r)$	Pore volume distribution function (m^3/m · kg)
V_p	Cumulative pore volume (m^3/kg)
x_i	Mole fraction of species i
X	Solid conversion at each time
y	Dimensionless position in the pellet
Z	Ratio of molar volume of solid product to solid reactant
β	Product layer resistance, $\frac{2k_{sB}\rho_B(1-\varepsilon_0)}{M_B D_P S_0}$
δ	Variation ratio of the pore diffusion
ε	Pellet porosity
ε_0	Initial pellet porosity
θ	Dimensionless bulk flow effect parameter, $(\vartheta_C - 1)x_{Ab}$
v_i	Stoichiometric coefficient of the reactant and product
ρ_B	True density of the solid reactant (kg/m^3)
ρ_D	True density of the solid product (kg/m^3)
τ	Dimensionless time
ϕ	Thiele modulus for the pellet, $\frac{L_0}{2}\sqrt{\frac{k_s\rho_B S_0}{M_B D_{e_0}}}$.

LITERATURE CITED

1. Houghton, J.T., Ding, Y., Griggs, D.J., Noguer, M., Van Der Linden, P.J., Dai, X., Maskell, K. & Johnson, C., Climate change 2001: the scientific basis, Cambridge University Press, UK, 2001.

2. Dean, C., Blamey, J., Florin, N., Al-Jeboori & M., Fennell, P. (2011). The calcium looping cycle for CO_2 capture from power generation, cement manufacture and hydrogen production. Chem. Eng. Res. Des. 89, 836–855. DOI: 10.1016/j.cherd.2010.10.013.

3. Abanades, J.C., Grasa, G., Alonso, M., Rodriguez, N., Anthony, E.J. & Romeo, L.M. (2007). Cost structure of a postcombustion CO_2 capture system using CaO. Environ. Sci. Technol. 41, 5523–5527. DOI: 10.1021/es070099a.

4. Abanades, J.C., Anthony, E.J., Wang, J. & Oakey, J.E. (2005). Fluidized bed combustion systems integrating CO_2 capture with CaO. Environ. Sci. Technol. 39, 2861–2866. DOI: 10.1021/es0496221.

5. Fang, F., Li, Z.S. & Cai, N.S. (2009). Continuous CO_2 capture from flue gases using a dual fluidized bed reactor with calcium-based sorbent. Ind. Eng. Chem. Res. 48, 11140–11147. DOI: 10.1021/ie901128r.

6. Shimizu, T., Hirama, T., Hosoda, H., Kitano, K., Inagaki, M., Tejima, K. (1999). A twin fluid-bed reactor for removal of CO_2 from combustion processes. Chem. Eng. Res. Des. 77, 62–68. DOI: 10.1205/026387699525882.

7. Bhatia, S.K. & Perlmutter, D.D. (1983). Effect of the product layer on the kinetics of the CO_2-lime reaction, AIChE J. 29, 79–86. DOI: 10.1002/aic.690290111.

8. Khoshandam, B., Kumar, R.V. & Allahgholi, L. (2010) Mathematical modeling of CO_2 removal using carbonation with CaO: The grain model. Kor. J. Chem. Eng. 27, 766–776. DOI: 10.1007/s11814-010-0119-5.

9. Sun, P., Grace, J.R., Lim, C.J., Anthony, E.J. (2008). Determination of intrinsic rate constants of the CaO–CO_2 reaction. Chem. Eng. Sci. 63, 47–56. DOI: 10.1016/j.ces.2007.08.055.

10. Sun, P., Grace, J.R., Lim, C.J. & Anthony, E.J. (2008). A discrete-pore-size-distribution-based gas–solid model and its application to the CaO-CO_2 reaction. Chem. Eng. Sci. 63, 57–70. DOI: 10.1016/j.ces.2007.08.055.

11. Nitsch, W. (1962). Über die Druckabhängigkeit der $CaCO_3$-Bildung aus dem Oxyd. Z. Elektrochem 66, 703–708. OI: 10.1002/bbpc.19620660821.

12. Dennis, J.S. & Hayhurst, A.N. (1987). The effect of CO_2 on the kinetics and extent of calcination of limestone and dolomite particles in fluidised beds. Chem. Eng. Sci. 42, 2361–2372. DOI: 10.1016/0009-2509(87)80110-0.

13. Grasa, G., Murillo, R., Alonso, M., Abanades, J.C. (2009). Application of the random pore model to the carbonation cyclic reaction. AIChE J. 55, 1246–1255. DOI: 10.1002/aic.11746.

14. Bhatia, S.K. & Perlmutter, D.D. (1981). A random pore model for fluid-solid reactions: II. Diffusion and transport effects. AIChE J. 27, 247–254. DOI: 10.1002/aic.690270211.

15. Wakao, N. & Smith, J.M. (1962). Diffusion in catalyst pellets. Chem. Eng. Sci. 17, 825–834. DOI: 10.1016/0009-2509(62)87015-8.

16. Slattery, J.C. & Bird, R.B. (1958). Calculation of the diffusion coefficient of dilute gases and of the self-diffusion coefficient of dense gases. AIChE J. 4, 137–142. DOI: 10.1002/aic.690040205.

17. Smith, J.M., Chemical engineering kinetics, McGraw-Hill, 1981.

18. Barker, R. (1973). The reversibility of the reaction $CaCO_3$, $CaO+CO_2$ J. Appl. Chem. Biotechnol. 23, 733–742. DOI: 10.1002/jctb.5020231005.

19. Kyaw, K., Kanamori, M., Matsuda, H., Hasatani, M. (1996). Study of Carbonation Reactions of Ca-Mg Oxides for High Temperature Energy Storage and Heat Transformation. J. Chem. Eng. Jpn. 29, 112–118. DOI: 10.1252/jcej.29.112.

20. Mess, D., Sarofim, A.F. & Longwell, J.P. (1999). Product layer diffusion during the reaction of calcium oxide with carbon dioxide. Energ Fuels 13, 999–1005. DOI: 10.1021/ef980266f.

21. Stendardo, S. & Foscolo, P.U. (2009). Carbon dioxide capture with dolomite: A model for gas–solid reaction within the grains of a particulate sorbent. Chem. Eng. Sci. 64, 2343–2352. DOI: 10.1016/j.ces.2009.02.009.

22. Anderson, T.F. (1969). Self-diffusion of carbon and oxygen in calcite by isotope exchange with carbon dioxide. J.Geophys. Res. 74, 3918–3932. DOI: 10.1029/JB074i015p03918.